JOURNAL OF EXPERIMENTAL AND THEORETICAL PHYSICS, 2025, Vol. 167, No. 1, pp. 24–41

ATOMS, MOLECULES, OPTICS

XUV-INDUCED CHANNELS FOR STIMULATED GENERATION OF RADIATION BY AN ATOM IN AN INTENSE IR LASER FIELD

© 2025 Ya. V. Breev[a, b], A. A. Minina[a, b], A. V. Flegel[a, b,*], M. V. Frolov[a, b,]**

[a] *Department of Physics, Voronezh State University, Voronezh, Russia*
[b] *Department of Radiophysics, Lobachevsky State University, Nizhny Novgorod, Russia*
**e-mail: flegel@cs.vsu.ru*
***e-mail: frolov@phys.vsu.ru*

Received September 13, 2024
Revised September 13, 2024
Accepted September 26, 2024

Abstract. The perturbation theory in interaction of isolated attosecond XUV pulse with an atomic system subjected to an intense IR field has been developed. Analytical expressions have been obtained for XUV-induced corrections to the wave function and amplitude of radiation generation in arbitrary order of perturbation theory. The contribution of partial amplitudes of radiation generation is analyzed for different channels with absorption of XUV photons at the ionization and recombination steps of the rescattering scenario. The region of **IR- and XUV-pulse** parameters are identified, in which interference of different XUV-induced channels is possible up to the third order of perturbation theory in XUV interaction.

Keywords: *isolated attosecond XUV-pulse, intense IR field, adiabatic approach, perturbation theory, high harmonic generation, rescattring effects*

DOI: 10.31857/S00444510250102e4

1. INTRODUCTION

Significant progress has been made in the theoretical description of nonlinear effects arising from the interaction of intense infrared (IR) laser fields with atomic systems. The quantum mechanical description of processes induced by an intense IR field involves two approaches: numerical methods, such as solving the time-dependent Schrödinger equation (TDSE) and its simplified variations for multi-electron systems (density functional theory, time-dependent Hartree-Fock method) [1–9], and analytical approaches. Numerical calculations typically serve as “benchmarks” for verifying the accuracy of analytical approaches and demonstrate their efficiency in determining the nonlinear response of an atomic system to an intense external alternating electric field. However, the results of numerical integration can only be obtained for fixed laser parameters and lack significant predictive power. Specifically, in most cases, it is necessary to perform numerous time-consuming computations to achieve the desired physical interpretation of the observed effect. In contrast, analytical theories are better suited for uncovering general fundamental patterns in the nonlinear interaction of an atomic system with an intense laser field.

Analytical approaches to describing nonlinear effects in the interaction of IR fields with atomic or molecular systems are typically based on the single-electron approximation. Within this approximation (subject to certain obvious limitations), it becomes possible to derive expressions for the amplitudes and cross sections of fundamental laser-induced and laser-assisted atomic processes with accuracy not inferior to numerical results of TDSE solution [10–16].

A key advantage of analytical approaches over numerical methods is the ability to establish a universal parameterization dependence of the probabilities of the strong-field processes on the fundamental characteristics of the target (i.e. the electron-core interaction potential $U(r)$) and the laser-pulse parameters (see, e.g., [17]).

These parameterizations can be further generalized to multi-electron systems, enabling the study of the effects of internal electronic dynamics in laser-induced photoprocesses [18].

Among the analytical approaches, the most popular is the S-matrix formalism, where the exact wave function of the active electron in the self-consistent potential $U(r)$ is expanded into a formal series in $U(r)$ [19, 20] (see also [21, 22]). This expansion leads to a Born series for the transition amplitude, where the terms (partial transition amplitudes) can be expressed as a convolution of the free-electron Green's function in the laser field with the atomic potential. For example, for the above-threshold ionization (ATI) process, the account of $U(r)$ in the lowest order leads to the Keldysh result [23].

Due to the large value of the classical action of the electron in a strong low-frequency field, the partial amplitudes can be analyzed using the saddle-point method [24], which gives rise to the quantum orbit approach [25, 26]. This approach provides an intuitive physical interpretation of strong-field phenomena in terms of classical trajectories, thereby justifying the rescattering model for fundamental atomic photoprocesses in an intense laser field [19, 20, 27, 28].

Although the Born expansion of transition amplitudes has proven fruitful and significantly contributes to the description of strong-field phenomena, it cannot fully account for the atomic potential, whose influence can be crucial [9, 18, 29–32]. One approach that allows for a more accurate treatment of the atomic system dynamics in an intense low-frequency field is the adiabatic approximation. The general idea of this approximation is based on the smallness of the carrier frequency ω of the laser pulse compared to the ionization threshold I_p of the atomic target $\hbar\omega \ll I_p$. The lowest-order of the adiabatic approximation (zero-order approximation) is defined by the quasistationary state of the system in a static (DC) field with an intensity equal to the instantaneous value of the low-frequency laser field [33–37]. In [11–17], a correction to the zero-order adiabatic approximation was derived for the wave function, accounting for the rescattering of the electron by the atomic potential. The study [38] refined the adiabatic approach for determining the atomic state in the lowest adiabatic approximation, by utilizing the analytical part of the wave function of the quasistationary atomic state in the instantaneous laser field. Within the adiabatic approach, both low-energy and high-energy (rescattering plateaus) parts of the photoelectron spectra and high-harmonic generation (HHG) spectra have been calculated.

The presence of a closed analytical expression for the wave function of the atomic state in an intense IR field allows for the development of an adiabatic perturbation theory in additional interaction with a high-frequency (e.g., extreme ultraviolet – XUV) attosecond pulse [17, 39]. The influence of an ultrashort XUV pulse on the radiation generation process results in the appearance of a significant number of new generation channels and substantial modification of the IR field HHG spectra. For example, the enhancement of harmonic yield due to the resonant population of excited target states by the XUV pulse was studied in [40–43]. XUV-induced enhancement of high harmonic yield was investigated both for attosecond pulse train [44–47] and for an isolated attosecond XUV pulse [48, 49]. These studies demonstrated that a XUV pulse (or its sequence) can affect the ionization stage in the three-step Corkum model [50], i.e., change the ionization times and thereby affect the harmonic yield. In [51, 52], it was shown that adding a weak XUV field leads to the appearance of an additional plateau in the HHG spectra. The physics of the additional XUV-induced plateau was explained in [53], where it was shown that the additional plateau results from XUV-photon absorption at the recombination stage. It should also be noted that, at sufficiently high carrier frequencies of the XUV pulse, electrons from the inner atomic shell can also participate in the HHG process, leading to an increase in the cutoff energy of the plateau [54–56]. Moreover, such XUV pulses, combined with an intense IR field, enable the study of Auger processes [57, 58] and electronic transitions from inner shells to the valence shell [59]. The re-emission channel (or elastic scattering) of a XUV photon by the atomic system, leading to significant enhancement of the generated radiation yield, was studied in [60]. Second-order processes of XUV interaction in an IR-dressed atomic medium were also investigated: generation of a XUV pulse at the doubled carrier frequency [39] and the XUV pulse rectification effect [61].

In this paper, we generalize the perturbative approach proposed in [17, 39] to construct perturbation theory corrections for the interaction with a short XUV pulse of arbitrary order, based on adiabatic wave functions of the atomic state in an intense IR field. Within the developed perturbation theory, XUV-induced radiation generation channels are investigated by analyzing classical electron trajectories in the field of synchronized intense IR and attosecond XUV pulses, and the possibility of interference between different channels due to their spectral overlap is explored. The article uses atomic units unless otherwise specified.

2. ADIABATIC APPROACH TO THE DESCRIPTION OF AN ATOM IN A LOW-FREQUENCY LASER FIELD

2.1. Adiabatic expression for the wave function

Let us consider the interaction of an atomic system with an intense infrared (IR) laser pulse characterized by the peak electric field strength F_{IR} and the carrier frequency ω_{IR}. We will assume that the laser pulse parameters satisfy the adiabatic conditions [23]:

$$\omega_{IR} \ll |E_0|, \quad \gamma_K \ll 1, \tag{1}$$

where $\gamma_K = \kappa\omega_{IR} / F_{IR}$ is the Keldysh parameter, $\kappa = \sqrt{2|E_0|}$, E_0 is related to the binding energy of the unperturbed atomic level. The conditions (1) can also be rewritten in terms of the average oscillation energy of a free electron in the laser field $u_p = F_{IR}^2 / (4\omega_{IR}^2)$:

$$\omega_{IR} \ll |E_0|, \quad \omega_{IR} \ll u_p. \tag{2}$$

To describe the nonlinear interaction of an atomic system with a laser field that satisfies the conditions (2), it is most convenient to use the adiabatic approach [12, 13, 37]. Within this approach, the wave function of an atomic electron interacting with a low-frequency laser field can be represented as a sum of "slow" ($\Psi_{IR}^{(0)}(\mathbf{r},t)$) and "fast" ($\Psi_{IR}^{(r)}(\mathbf{r},t)$) time-dependent parts [11, 12, 17]:

$$\Psi_{IR}(\mathbf{r},t) = \Psi_{IR}^{(0)}(\mathbf{r},t) + \Psi_{IR}^{(r)}(\mathbf{r},t). \tag{3}$$

The slow part $\Psi_{IR}^{(0)}(\mathbf{r},t)$ represents the adiabatic approximation in the lowest order ("zero-order" approximation) and is defined by the quasistationary state in a DC electric field with a strength equal to the instantaneous value of the IR field at time t [37, 12]. In many practical calculations, the function $\Psi_{IR}^{(0)}(\mathbf{r},t)$ can be accurately approximated by the initial-state wave function in the absence of the IR field:

$$\Psi_{IR}^{(0)}(\mathbf{r},t) \approx e^{-iE_0t}\varphi_0(\mathbf{r}). \tag{4}$$

The term $\Psi_{IR}^{(r)}(\mathbf{r},t)$ in Eq. (3) describes the rescattering effects of the valence electron on the atomic core and represents a superposition of scattering states $\psi_{\mathbf{K}_s}^{(+)}$ of the electron in the atomic potential with laser-induced momenta $\mathbf{K}_s$ [17]:

$$\Psi_{IR}^{(r)}(\mathbf{r},t) = e^{-iE_0t}\Phi_{IR}^{(r)}(\mathbf{r},t), \tag{5a}$$

$$\Phi_{IR}^{(r)}(\mathbf{r},t) = \sum_s a_s(t)\psi_{\mathbf{K}_s}^{(+)}(\mathbf{r}). \tag{5b}$$

Each term in the sum (5b) is associated with one of the possible closed classical trajectories, which start at the tunneling time t_s' and end at the return time t of the electron back to the atomic core. The laser-induced momenta are defined by the expression:

$$\mathbf{K}_s = \mathbf{K}(t,t_s'), \tag{6}$$

$$\mathbf{K}(t,t') = \mathbf{A}_{IR}(t) - \frac{1}{t-t'}\int_{t'}^{t}\mathbf{A}_{IR}(\tau)d\tau,$$

where $\mathbf{A}_{IR}(t)$ is the vector potential associated with the electric field strength $\mathbf{F}_{IR}(t)$ of the laser pulse by the relation:

$$\mathbf{F}_{IR}(t) = -\partial\mathbf{A}_{IR}(t) / \partial t.$$

The tunneling times $t_s'(t)$ as functions of the return times t satisfy the transcendental equation (see details in [14]):

$$\mathbf{K}_s' \cdot \dot{\mathbf{K}}_s' = 0, \tag{7}$$

where

$$\mathbf{K}_s' \equiv \mathbf{K}'(t,t_s'),$$
$$\dot{\mathbf{K}}_s' = \frac{\partial\mathbf{K}_s'}{\partial t_s'}, \tag{8}$$
$$\mathbf{K}'(t,t') = \mathbf{A}_{IR}(t') - \frac{1}{t-t'}\int_{t'}^{t}\mathbf{A}_{IR}(\tau)d\tau.$$

Equation (7) has a simple physical meaning: the atomic electron tunnels at the moments in time that provide the minimum kinetic energy of the released electron in the laser field. The time-dependent coefficients $a_s(t)$ in the superposition (5b) represent the product of the ionization (tunneling) factor $a^{(tun)}(t'_s)$ and the propagation factor $a^{(pr)}(t,t'_s)$:

$$a_s(t) = a^{(tun)}(t'_s)\,a^{(pr)}(t,t'_s). \tag{9}$$

The ionization factor is characterized by the tunneling exponent in the instantaneous "static" electric field with the strength:

$$\mathcal{F} = [\mathbf{F}^2_{IR}(t'_s) - \mathbf{K}'_s \cdot \dot{\mathbf{F}}_{IR}(t'_s)]^{1/2},$$

see [62]. For example, in the case of a linearly polarized laser field, the following relation holds:

$$a^{(tun)}(t'_s) \propto e^{-F_{at}/(3|F_{IR}(t'_s)|)}, \tag{10}$$

where $F_{at} = \kappa^3$ defines the magnitude of the characteristic intra-atomic field. To satisfy the quasiclassical condition, an additional inequality must hold: $F \ll F_{at}$, which ensures the smallness of the ionization factor and the insignificance of the initial-state decay effects.

The propagation factor $a^{(pr)}(t,t'_s)$ is determined by the classical action $S(t,t'_s)$ of the free electron in the laser field over the time interval from t'_s to t:

$$a^{(pr)}(t,t'_s) = \frac{e^{iE_0(t-t'_s)-iS(t,t'_s)}}{(t-t'_s)^{3/2}}, \tag{11a}$$

$$S(t,t'_s) = \frac{1}{2}\int_{t'_s}^{t}\Big[\mathbf{A}_{IR}(\tau) - \frac{1}{t-t'_s}\int_{t'_s}^{t}\mathbf{A}_{IR}(\tau')d\tau'\Big]^2 d\tau. \tag{11b}$$

It is important to note that the rescattered part $\Phi^{(r)}_{IR}(\mathbf{r},t)$ of the atomic electron wave function in the IR field, relative to the unperturbed function $\varphi_0(\mathbf{r})$, has a smallness $\sim \beta_{IR}$

$$\beta_{IR} = \gamma_K^{3/2}\frac{F_{IR}}{F_{at}}e^{-F_{at}/(3F_{IR})} \ll 1.$$

Essentially, the result (3) represents an expansion of the atomic electron state in terms of β_{IR} up to the first order. In the following, we will maintain this accuracy, as the inclusion of higher-order terms in the expansion of β_{IR} (i.e., a more precise account of rescattering effects) does not lead to any significant manifestations in the amplitudes and cross sections of processes in a strong IR laser field.

2.2 Amplitude of radiation generation

The amplitude of photon generation by an atom in an intense laser field is determined by the dipole matrix element [63, 64]:

$$\mathbf{D}(\Omega) = \int\langle\tilde{\Psi}_{IR}(\mathbf{r},t)|\mathbf{r}|\Psi_{IR}(\mathbf{r},t)\rangle e^{i\Omega t}dt, \tag{12}$$

where Ω is the frequency of the generated photon, $\tilde{\Psi}_{IR}(\mathbf{r},t)$ is the dual wave function to the state $\Psi_{IR}(\mathbf{r},t)$, defined from the state $\Psi_{IR}(\mathbf{r},t)$ by complex conjugation, time reversal $t \to -t$, and the replacement of all t-odd parameters λ for $-\lambda$ [65, 66]. In a low-frequency laser field, the dipole matrix element (12) for $\Omega > |E_0|$ can be approximately expressed through $\Psi^{(0)}(\mathbf{r},t)$ and $\Psi^{(r)}_{IR}(\mathbf{r},t)$ [17, 63]:

$$\mathbf{D}(\Omega) = \int\langle\varphi_0 e^{-iE_0 t} \mid \mathbf{r} \mid \Psi^{(r)}_{IR}(\mathbf{r},t)\rangle e^{i\Omega t}dt. \tag{13}$$

The harmonic yield, summed over polarizations and integrated over directions, is determined by the square of the modulus of $\mathbf{D}(\Omega)$:

$$Y = \frac{\Omega^4|\mathbf{D}(\Omega)|^2}{4\pi^2 c^3},$$

where c is the speed of light.

In the adiabatic approximation, the time integral in (13) is evaluated using the saddle-point method, and $\mathbf{D}(\Omega)$ can be represented as a sum of partial amplitudes $\mathbf{D}_j(\Omega)$ [14, 17]:

$$\mathbf{D}(\Omega) = \sum_j \mathbf{D}_j(\Omega), \tag{14a}$$

$$\mathbf{D}_j(\Omega) = a_j^{(tun)}\bar{a}_j\mathbf{d}(\mathbf{K}_j)e^{i\Omega t_j}, \tag{14b}$$

where $a_j^{(tun)}$, $\bar{a}_j$ are the tunneling and propagation factors, respectively, and $\mathbf{d}(\mathbf{K}_j)$ is the dipole matrix element for the transition from the continuum state with momentum $\mathbf{K}_j$ to the bound state $\varphi_0(\mathbf{r})$:

$$\mathbf{d}(\mathbf{K}_j) = \langle\varphi_0(\mathbf{r}) \mid \mathbf{r} \mid \psi^{(+)}_{\mathbf{K}_j}(\mathbf{r})\rangle.$$

The factors $a_j^{(tun)}$, $\bar{a}_j$ are defined by the relations:

$$a_j^{(tun)} \equiv a^{(tun)}(t'_j),$$

$$\bar{a}_j = \sqrt{\frac{2\pi i}{\mathbf{K}_j \cdot \mathbf{F}_{IR}(t_j) + \dfrac{\mathbf{K}_j^2}{t_j - t'_j}}}\,a^{(pr)}(t_j,t'_j).$$

The summation in (14a) is performed over all closed classical electron trajectories, defined by the start time t'_j and end time t_j of the electron's motion. The times t'_j and t_j are the roots of the system of transcendental equations [14, 17]:

$$\mathbf{K}'_j \cdot \dot{\mathbf{K}}'_j = 0, \quad \mathbf{K}_j^2 = 2(\Omega + E_0), \tag{15}$$

where the induced momenta $\mathbf{K}'_j \equiv \mathbf{K}'(t_j, t'_j)$, $\mathbf{K}_j \equiv \mathbf{K}(t_j, t'_j)$ are defined in Eqs. (8) and (6), respectively.

3. TIME-DEPENDENT PERTURBATION THEORY FOR AN ATOMIC SYSTEM IN AN INTENSE IR FIELD

Let us consider an atomic system interacting with an intense IR field and a perturbative XUV pulse. The account of the XUV interaction with the IR-dressed atomic system can be treated within the perturbation theory based on the adiabatic wave functions of the atomic electron in the IR field [17]. We will consider the interaction with the XUV pulse in the dipole approximation, so that the potential $V_{XUV}(\mathbf{r},t)$ of the interaction between the atomic electron and the XUV pulse has the form:

$$V_{XUV}(\mathbf{r},t) = V_+(\mathbf{r},t)e^{-i\omega_{XUV}t} + V_-(\mathbf{r},t)e^{i\omega_{XUV}t}, \tag{16}$$

$$V_+(\mathbf{r},t) = \frac{F_{XUV}}{2}(\mathbf{e}_{XUV} \cdot \mathbf{r}) f_{XUV}(t),$$

$$V_-(\mathbf{r},t) = V_+^*(\mathbf{r},t),$$

where F_{XUV} is the peak field strength, ω_{XUV} is the carrier frequency, $\mathbf{e}_{XUV}$ is the polarization vector, and $f_{XUV}(t)$ is the XUV pulse envelope.

Note that for $\omega_{XUV} > |E_0|$, the small perturbation parameter for the XUV interaction is defined as [67]

$$\beta_{XUV} = \frac{\kappa F_{XUV}}{\omega_{XUV}^2} = 4\frac{|E_0|^2}{\omega_{XUV}^2}\frac{F_{XUV}}{F_{at}} \ll 1. \tag{17}$$

Therefore, even in the case of XUV radiation strength comparable to F_{at}, the interaction V_{XUV} can be treated perturbatively [68].

The state $\Psi(\mathbf{r},t)$ of the atomic electron in the field of synchronized IR and XUV pulses can be written as:

$$\Psi(\mathbf{r},t) = \Psi_{IR}(\mathbf{r},t) + \\ + \iint \mathcal{G}(\mathbf{r},t;\mathbf{r}',t') V_{XUV}(\mathbf{r}',t') \Psi_{IR}(\mathbf{r}',t') d\mathbf{r}' dt', \tag{18}$$

where $\mathcal{G}(\mathbf{r},t;\mathbf{r}',t')$ is the time-dependent (retarded) Green's function of the atomic electron in the two-component field. For the function $\mathcal{G}(\mathbf{r},t;\mathbf{r}',t')$, the Dyson equation holds:

$$\mathcal{G}(\mathbf{r},t;\mathbf{r}',t') = \mathcal{G}_{IR}(\mathbf{r},t;\mathbf{r}',t') + \iint \mathcal{G}_{IR}(\mathbf{r},t;\mathbf{r}'',t'') \times \\ \times V_{XUV}(\mathbf{r}'',t'') \mathcal{G}(\mathbf{r}'',t'';\mathbf{r}',t') d\mathbf{r}'' dt'', \tag{19}$$

where $\mathcal{G}_{IR}(\mathbf{r},t;\mathbf{r}',t')$ is the time-dependent (retarded) Green's function of the atomic electron in the IR field. Using the relations (18) and (19), we can represent the wave function $\Psi(\mathbf{r},t)$ as a perturbation series in V_{XUV}:

$$\Psi(\mathbf{r},t) = \Psi_0(\mathbf{r},t) + \sum_{n=1}^{\infty} \Psi_n(\mathbf{r},t), \tag{20}$$

where $\Psi_0(\mathbf{r},t) \equiv \Psi_{IR}(\mathbf{r},t)$ is the atomic state in the absence of the XUV pulse (see Eq. (3)), and $\Psi_n(\mathbf{r},t) \sim \beta_{XUV}^n$ are the n-order corrections, satisfying the following recursive relation:

$$\Psi_{n+1}(\mathbf{r},t) = \iint \mathcal{G}_{IR}(\mathbf{r},t;\mathbf{r}',t') \times \\ \times V_{XUV}(\mathbf{r}',t') \Psi_n(\mathbf{r}',t') d\mathbf{r}' dt'. \tag{21}$$

The accuracy of the adiabatic approximation allows for the approximate evaluation of the time integrals in (21). The main contribution to the value of the corresponding integrals are given primarily by the weakly overlapping neighborhoods of the points $t' = t$ and $t' = \tilde{t}'_s(t)$, where $\tilde{t}'_s(t)$ are the saddle points of the phase of the rapidly oscillating factor of the integrand in (21). This phase is primarily determined by the classical action of the electron in the IR field and the carrier frequency of the XUV pulse. The asymptotic expression for the Green's function $\mathcal{G}_{IR}(\mathbf{r},t;\mathbf{r}',t')$ in the vicinity of these singular points was obtained in [17]:

$$\mathcal{G}_{IR}(\mathbf{r},t;\mathbf{r}',t') \approx \\ \approx \begin{cases} G_{at}(\mathbf{r},t;\mathbf{r}',t'), & t \approx t', \\ G_{vol}(0,t;0,t')\psi_{\mathbf{K}}^{(+)}(\mathbf{r})[\psi_{\mathbf{K}'}^{(+)}(\mathbf{r}'')]^*, & t \neq t', \end{cases} \tag{22}$$

Where $G_{at}(\mathbf{r},t;\mathbf{r}',t')$ is the time-dependent atomic Green's function of the electron, $G_{vol}(0,t;0,t')$ is the Volkov Green's function of the electron in the IR field for $\mathbf{r} = \mathbf{r}' = 0$, and the momenta $\mathbf{K} \equiv \mathbf{K}(t,t')$ and $\mathbf{K}' \equiv \mathbf{K}'(t,t')$ are defined by Eq. (6) and (8), respectively.

The explicit expression for the nth-order correction $\Psi_n(\mathbf{r},t)$ can be obtained by sequentially calculating the lower-order corrections, using the relations (22) and (21) and approximately evaluating the time integrals. The nth-order correction can be decomposed into a slow part $\Psi_n^{(s)}$ and a fast part $\Psi_n^{(r)}$:

$$\Psi_n(\mathbf{r},t') = \Psi_n^{(s)}(\mathbf{r},t') + \Psi_n^{(r)}(\mathbf{r},t'). \qquad (23)$$

To determine the slow part $\Psi_n^{(s)}$, we represent it as a superposition:

$$\Psi_n^{(s)}(\mathbf{r},t) \approx \sum_{\nu} e^{-iE_\nu t}\varphi_\nu^{(n)}(\mathbf{r},t), \qquad (24)$$

where $E_\nu = E_0 + \nu\omega_{XUV}$ are time-dependent coefficients, and the slow (in time) functions $\varphi_\nu^{(n)}(\mathbf{r},t)$ require further definition. The slow time dependence of the functions $\varphi_\nu^{(n)}(\mathbf{r},t)$, as well as the envelope $f_{XUV}(t)$, will be understood under the following conditions:

$$\left|\frac{\partial\varphi_\nu^{(n)}}{\partial t}\right| \ll \omega_{XUV}\left|\varphi_\nu^{(n)}\right|, \qquad (25a)$$

$$\left|\frac{\partial f_{XUV}(t)}{\partial t}\right| \ll \omega_{XUV}\left|f_{XUV}(t)\right|. \qquad (25b)$$

It should be emphasized that in order to isolate the slowly varying part of the wave function, one should neglect the contribution from the saddle point neighborhoods $\tilde{t}_s'(t)$ in the time integral in (21) and consider only the vicinity of the endpoint $t' \approx t$. Substituting (24) into (21) and using the asymptotic form of the Green's function for $t' \to t$ (see Eq. (22)), we obtain:

$$\sum_{\nu} e^{-iE_\nu t}\varphi_\nu^{(n+1)}(\mathbf{r},t) = \iint G_{at}(\mathbf{r},t;\mathbf{r}',t')\times$$
$$\times V_{XUV}(\mathbf{r}',t')\sum_{\nu'} e^{-iE_{\nu'}t'}\varphi_{\nu'}^{(n)}(\mathbf{r}',t')d\mathbf{r}'dt'. \qquad (26)$$

Next, approximating the slow functions $\varphi_\nu^{(n)}(\mathbf{r}',t')$ on the right-hand side of Eq. (26) by their values at $t' = t$ and using the relation between the stationary and time-dependent atomic Green's functions:

$$G_E(\mathbf{r},\mathbf{r}') = \int e^{iE(t-t')}G_{at}(\mathbf{r},t;\mathbf{r},t')dt', \qquad (27)$$

we obtain:

$$\sum_{\nu} e^{-iE_\nu t}\varphi_\nu^{(n+1)}(\mathbf{r},t) =$$
$$= \sum_{\nu'} e^{-iE_{\nu'+1}t}G_{E_{\nu'+1}}V_+ \mid \varphi_{\nu'}^{(n)}\rangle +$$
$$+\sum_{\nu'} e^{-iE_{\nu'-1}t}G_{E_{\nu'-1}}V_- \mid \varphi_{\nu'}^{(n)}\rangle. \qquad (28)$$

Note that if the energy of the Green's function coincides with the energy of the ground state, then, according to perturbation theory, the Green's function is replaced by the reduced Green's function G'_{E_0} [69, 70]:

$$G'_{E_0} = \lim_{E\to E_0}\left[G_E(\mathbf{r},\mathbf{r}') - \frac{\varphi_0^*(\mathbf{r}')\varphi_0(\mathbf{r})}{E - E_0}\right]. \qquad (29)$$

Given the weak dependence of the functions $\varphi_{\nu'}^{(n)}$ and $V_\pm$ on time [see (25)], we equate the coefficients of the "fast-oscillating" exponentials with identical exponents in (32) and obtain the equation for the functions $\varphi_\nu^{(n+1)}$:

$$\varphi_\nu^{(n+1)} = \begin{cases} G_{E_\nu}V_+ \mid \varphi_{\nu-1}^{(n)}\rangle + G_{E_\nu}V_- \mid \varphi_{\nu+1}^{(n)}\rangle, & \nu \neq 0, \\ G'_{E_0}V_+ \mid \varphi_{-1}^{(n)}\rangle + G'_{E_0}V_- \mid \varphi_{+1}^{(n)}\rangle, & \nu = 0. \end{cases} \qquad (30)$$

The iterative method for solving Eq. (30) assumes the following expression for the zero iteration:

$$\varphi_\nu^{(0)}(\mathbf{r},t) = \varphi_0(\mathbf{r})\delta_{\nu,0}. \qquad (31)$$

Thus, using the relations (24) and (30), one can find the nth-order correction for the slow part of the wave function, which formally coincides with the expression for the nth-order perturbation theory in a monochromatic field [70] (for a monochromatic field: $f_{XUV}(t) \equiv 1$, i.e., $V_\pm$ do not depend on time). We write the wave function $\Psi_n^{(s)}$ in the nth order of perturbation theory using the integral operator $\widehat{P}_n$:

$$\Psi_n^{(s)}(\mathbf{r},t) = \widehat{P}_n(E_0,t)\mid\varphi_0\rangle, \qquad (32)$$

which represents the convolution of the atomic Green's function with all possible n-combinations of the operators V_+ and/or V_-. We present the explicit form of the operators $\widehat{P}_n$ for the first three orders of perturbation theory ($n \leqslant 3$):

$$\widehat{P}_0(E_0,t) = e^{-iE_0t}\hat{I},$$

$$\widehat{P}_1(E_0,t) = e^{-iE_1t}G_{E_1}V_+ + e^{-iE_{-1}t}G_{E_{-1}}V_-,$$

$$\widehat{P}_2(E_0,t) = e^{-iE_2t}G_{E_2}V_+G_{E_1}V_+ +$$
$$+e^{-iE_0t}G'_{E_0}V_-G_{E_1}V_+ +$$

$$+e^{-iE_0t}G'_{E_0}V_+G_{E_{-1}}V_- +$$

$$+e^{-iE_{-2}t}G_{E_{-2}}V_-G_{E_{-1}}V_-,$$

$$\widehat{P}_3(E_0,t) = e^{-iE_3t}G_{E_3}V_+G_{E_2}V_+G_{E_1}V_+$$

$$+e^{-iE_1t}G_{E_1}V_-G_{E_2}V_+G_{E_1}V_+ +$$

$$+e^{-iE_1t}G_{E_1}V_+G'_{E_0}V_-G_{E_1}V_+ +$$

$$+e^{-iE_1t}G_{E_1}V_+G'_{E_0}V_+G_{E_{-1}}V_- +$$

$$+e^{-iE_{-1}t}G_{E_{-1}}V_-G'_{E_0}V_-G_{E_1}V_+ +$$

$$+e^{-iE_{-1}t}G_{E_1}V_-G'_{E_0}V_+G_{E_{-1}}V_- +$$

$$+e^{-iE_{-1}t}G_{E_{-1}}V_+G_{E_{-2}}V_-G_{E_{-1}}V_- +$$

$$+e^{-iE_{-3}t}G_{E_{-3}}V_-G_{E_{-2}}V_-G_{E_{-1}}V_-,$$

where $\widehat{I}$ is the identity operator. It is evident that the slow part of the wave function is the sum of partial terms $\Psi_n^{(s)}(\mathbf{r},t)$:

$$\Psi^{(s)}(\mathbf{r},t) = \sum_{n=0}^{\infty}\Psi_n^{(s)}(\mathbf{r},t) = \sum_{n=0}^{\infty}\widehat{P}_n(E_0,t)\varphi_0(\mathbf{r}). \quad (33)$$

The similarity between the perturbation series in the XUV interaction of the atomic wave function in an intense IR field and the well-known perturbation result for the quasistationary atomic state in a monochromatic laser field, obtained within the quasistationary quasienergy state (QQES) method [70], is noteworthy. The series (33) formally coincides with the QQES result after replacing the exact quasienergy ε by the ground state energy E_0 and the field strength F_{XUV} by the instantaneous amplitude of the pulse field $\mathcal{F}_{XUV}(t) = F_{XUV}f_{XUV}(t)$. Thus, if the functional dependence of the QQES wave function $\Psi_{XUV}^{(QQES)}(\mathbf{r},t;\varepsilon,F_{XUV})$ on the quasienergy and field strength is known, the same dependence defines the wave function $\Psi^{(s)}(\mathbf{r},t)$:

$$\Psi^{(s)}(\mathbf{r},t) = \Psi_{XUV}^{(QQES)}(\mathbf{r},t;E_0,\mathcal{F}_{XUV}(t)). \quad (34)$$

In contrast to the slow part, the time dependence of the fast part $\Psi_n^{(r)}(\mathbf{r},t)$ is determined by the rapidly oscillating exponential factor $\sim e^{-iS}$, defined by the classical action S of the electron in the IR field along the closed trajectories (see Eqs. (5b), (9), and (11a)). It should be noted that, within the adiabatic approximation, the appearance of any products of two or more Volkov Green's functions exceeds the accuracy of the method. Therefore, in any order of perturbation theory for the XUV interaction, the expression for $\Psi_n^{(r)}(\mathbf{r},t)$ contains only one Volkov Green's function. From relation (21), it follows that $\Psi_n^{(r)}(\mathbf{r},t)$ is defined as the convolution result of either the slow part $\Psi_n(\mathbf{r},t)$ with the Green's function G_{IR}, approximated by the Volkov Green's function (see Eq. (22), or the fast part $\Psi_n(\mathbf{r},t)$ with the Green's function G_{IR}, approximated by the atomic Green's function (see Eq. (22)):

$$\Psi_{n+1}^{(r)}(\mathbf{r},t) =$$

$$= \int G_{vol}(0,t;0,t')\langle\psi_{\mathbf{K}'}^{(+)}\,|\,V_{XUV}(t')\,|\,\Psi_n^{(s)}(t')\rangle\psi_{\mathbf{K}}^{(+)}(\mathbf{r})dt' +$$

$$+\iint G_{at}(\mathbf{r},t;\mathbf{r}',t')V_{XUV}(\mathbf{r}',t')\Psi_n^{(r)}(\mathbf{r}',t')d\mathbf{r}'dt', \quad (35)$$

where the first integral implies an approximate evaluation using the saddle-point method, while the second integral should be evaluated considering only the contribution from the vicinity of $t' \approx t$. Accordingly, $\Psi_{n+1}^{(r)}$ can be written as the sum of two terms:

$$\Psi_{n+1}^{(r)} = \Psi_{n+1}^{(r,1)} + \Psi_{n+1}^{(r,2)}, \quad (36)$$

where the expressions for для $\Psi_{n+1}^{(r,1)}$, $\Psi_{n+1}^{(r,2)}$ are discussed below.

We will use the approximate expression (27) for the Green's function $\Psi_n^{(s)}$ in the first integral of (39) and then perform the saddle-point integration over t'. As a result, we obtain an expression for $\Psi_{n+1}^{(r,1)}$:

$$\Psi_{n+1}^{(r,1)}(\mathbf{r},t) = {\sum_{\nu}}'\sum_{\tilde{t}'}\psi_{\tilde{\mathbf{K}}}^{(+)}(\mathbf{r})G_{\nu}(t,\tilde{t}')\times$$

$$\times\Big[\langle\psi_{\tilde{\mathbf{K}}'}^{(+)}\,|\,V_+(\tilde{t}')\,|\,\varphi_{\nu-1}^{(n)}\rangle + \langle\psi_{\tilde{\mathbf{K}}'}^{(+)}\,|\,V_-(\tilde{t}')\,|\,\varphi_{\nu+1}^{(n)}\rangle\Big], \quad (37)$$

where $\tilde{\mathbf{K}}' = \mathbf{K}'(t,\tilde{t}')$, $\tilde{\mathbf{K}} = \mathbf{K}(t,\tilde{t}')$, the summation is carried out over all allowed values of v with the same parity as $n+1$ in the interval $|\nu| \leqslant n+1$, and the saddle points $\tilde{t}' \equiv \tilde{t}'(t)$, defined by the equation:

$$\tilde{\mathbf{K}}'^2 = 2E_{\nu}. \quad (38)$$

In (37), the following notation is used, defined as:

$$G_{\nu}(t,\tilde{t}') = -\frac{e^{-iS(t,\tilde{t}')-iE_{\nu}\tilde{t}'}}{2\pi(t-\tilde{t}')^{3/2}}\times$$

$$\times\Big[\tilde{\mathbf{K}}'\cdot\mathbf{F}_{IR}(\tilde{t}') - 2E_{\nu}\,/\,(t-\tilde{t}')\Big]^{-1/2}. \quad (39)$$

The accuracy of the approximate expression for the Green's function in (22) implies that only those saddle points ν should be considered in the sum (37) that ensure the solution of Eq. (38) in real numbers.

From expression (37), it follows that the correction $\Psi_{n+1}^{(r,1)}$ to the fast part of the wave function describes a rescattering state, formed within the three-step scenario:

First stage: as a result of the absorption or emission of n XUV photons, the atomic system forms states $\varphi_{\nu}^{(n)}$.

Second stage: a stimulated single-photon transition (with absorption or emission of a photon) from one of the states $\varphi_{\nu}^{(n)}$ to a continuum state with asymptotic momentum $\tilde{\mathbf{K}}'$ occurs at the moment $\tilde{t}'$.

Third stage: while in the continuum, the electron interacts with the intense IR field and forms, at the moment t, the state $\psi_{\tilde{\mathbf{K}}}^{(+)}(\mathbf{r})$, acquiring energy while moving along a closed classical trajectory. The propagation of the electron wave packet in the continuum is described by the multiplier $G_{\nu}(t,\tilde{t}')$.

As follows from Eqs. (5b) and (37), the fast part of the wave function is determined by the rapidly oscillating factor $e^{-iS(t,t')}$, which defines the IR-controlled propagation of the electron in the continuum, and the continuum state function $\psi_{\mathbf{K}}^{(+)}$. The same components determine the correction $\Psi_n^{(r,2)}$, so, without loss of generality, we represent $\Psi_n^{(r,2)}$ as:

$$\Psi_n^{(r,2)} = \sum_s \hat{a}_s^{(n)}(t) \mid \psi_{\mathbf{K}_s}^{(+)}\rangle, \tag{40}$$

where $\hat{a}_s^{(n)}(t) \propto e^{-iS(t,\hat{t}'_s)}$ is a certain integral operator, and the summation is performed over all real ionization moments $\hat{t}'_s$, induced by the IR or XUV field. In the zero approximation for the XUV interaction: $\hat{t}'_s \equiv t'_s$ (see relation (7)), and $\hat{a}_s^{(0)} \equiv a_s(t)\hat{I}$ (see relation (9)). It is worth noting that the operator $\hat{a}_s^{(n)}(t)$ can be defined by two terms (denoted below by the indices a and b), describing two different scenarios of the electron interaction with the IR and XUV pulses:

a) The atomic electron tunnels into the IR-modified continuum and, while propagating along closed classical trajectories in the IR field, absorbs ν and emits $n-\nu$ of XUV photons (parity of n and ν is the same).

b) The atomic electron transitions into the IR-modified continuum with energy $E_{\nu'}$ by absorbing ν' of XUV photons, where, during propagation along the closed classical trajectories in the IR field, it absorbs and emits additional XUV photons.

According to the described mechanisms, we represent the function $\Psi_n^{(r,2)}$ as a sum:

$$\Psi_n^{(r,2)} = \Psi_n^{(r,2\mathrm{a})} + \Psi_n^{(r,2\mathrm{b})}. \tag{41}$$

The mathematical expression for the operator $\hat{a}_s^{(n)}(t)$, corresponding to the realization of Scenario (a), can be easily obtained from (35) (see the second integral term on the right-hand side), assuming that the "zero iteration" $\Psi_0^{(r)} = \Psi_{IR}^{(r)}$ for the fast part of the wave function is defined in (5). By sequentially calculating the time integrals in (35) and considering the contribution from the vicinity of the point $t' = t$, we obtain the general expression for $\Psi_n^{(r,2\mathrm{a})}(\mathbf{r},t)$:

$$\Psi_n^{(r,2\mathrm{a})}(\mathbf{r},t) = \sum_s a_s(t)\hat{P}_n\left(\frac{\mathbf{K}_s^2}{2},t\right)\psi_{\mathbf{K}_s}^{(+)}(\mathbf{r}), \tag{42}$$

where the summation includes all solutions of Eq. (7). It is worth noting that, similar to the previously considered case of the functions $\Psi^{(s)}(\mathbf{r},t)$, the summation of the perturbation series in n, taking into account the explicit form of (46), leads to a result formally coinciding with the expression for the quasienergy scattering state $\Psi_{\mathbf{K}}^{(+)}(\mathbf{r},t;\varepsilon,\mathcal{F}_{XUV}(t))$ of the atomic electron in a monochromatic XUV field [70] with the quasienergy $\varepsilon = \mathbf{K}_s^2/2$, the asymptotic momentum $\mathbf{K} = \mathbf{K}_s$, and the XUV field strength, equal to the instantaneous value $\mathcal{F}_{XUV}(t)$:

$$\sum_n \hat{P}_n\left(\frac{\mathbf{K}_s^2}{2},t\right)\psi_{\mathbf{K}_s}^{(+)}(\mathbf{r}) =$$

$$= \Psi_{\mathbf{K}_s}^{(+)}\left(\mathbf{r},t;\frac{\mathbf{K}_s^2}{2},\mathcal{F}_{XUV}(t)\right) \equiv \Psi_{\mathbf{K}_s}^{(+)}(\mathbf{r},t), \tag{43}$$

and therefore,

$$\Psi^{(r,2\mathrm{a})}(\mathbf{r},t) = \sum_n \Psi_n^{(r,2\mathrm{a})}(\mathbf{r},t) = \sum_s a_s(t)\Psi_{\mathbf{K}_s}^{(+)}(\mathbf{r},t). \tag{44}$$

The correction $\Psi_n^{(r,2\mathrm{b})}$ to the fast part of the wave function, responsible for the realization of Scenario (b), arises in the second and higher orders of perturbation theory. As the "zero iteration" for obtaining this correction, we use the term $\Psi_1^{(r,1)}$ ($\Psi_0^{(r)} = \Psi_1^{(r,1)}$), corresponding to the absorption of a XUV photon (see the first term in the square brackets in (37)):

$$\Psi_0^{(r)}(\mathbf{r},t) = \sum_{\tilde{t}'} \psi_{\tilde{\mathbf{K}}}^{(+)}(\mathbf{r}) G_1(t,\tilde{t}') \langle \psi_{\tilde{\mathbf{K}}'}^{(+)} \mid V_+(\tilde{t}') \mid \varphi_0 \rangle, \quad (45)$$

where $\tilde{t}'$ is determined from Eq. (38) with $\nu = 1$. Substituting (45) into the second term in (35) and evaluating the time integral in the vicinity of $t' \approx t$, we obtain the desired second-order correction:

$$\Psi_2^{(r,2\mathrm{b})}(\mathbf{r},t) = \sum_{\tilde{t}'} \widehat{P}_1\left(\frac{\tilde{\mathbf{K}}^2}{2}, t\right) \psi_{\tilde{\mathbf{K}}}^{(+)}(\mathbf{r}) \times$$

$$\times G_1(t,\tilde{t}') \langle \psi_{\tilde{\mathbf{K}}'}^{(+)} \mid V_+(\tilde{t}') \mid \varphi_0 \rangle. \quad (46)$$

It is easy to give a transparent physical meaning to relation (46): the electron, being in the bound state, absorbs a XUV photon and passes to a continuum state with asymptotic momentum $\tilde{\mathbf{K}}'$ (that corresponds to the matrix element $\langle \psi_{\tilde{\mathbf{K}}'}^{(+)} \mid V_+(\tilde{t}') \mid \varphi_0 \rangle$ in (46)). The electron propagates in the IR-dressed continuum along a closed trajectory (see the multiplier $G_1(t,\tilde{t}')$). As a result, it forms a continuum state at time t through a single-photon channel of interaction with XUV radiation (i.e., by absorbing or emitting a XUV photon).

In the third order of perturbation theory, the calculations are carried out similarly, and the corresponding correction takes the form:

$$\Psi_3^{(r,2\mathrm{b})}(\mathbf{r},t) = \sum_{\tilde{t}'(\nu=1)} \widehat{P}_2\left(\frac{\tilde{\mathbf{K}}^2}{2}, t\right) \psi_{\tilde{\mathbf{K}}}^{(+)}(\mathbf{r}) \times$$

$$\times G_1(t,\tilde{t}') \langle \psi_{\tilde{\mathbf{K}}'}^{(+)} \mid V_+(\tilde{t}') \mid \varphi_0 \rangle +$$

$$+ \sum_{\tilde{t}'(\nu=2)} \widehat{P}_1\left(\frac{\tilde{\mathbf{K}}^2}{2}, t\right) \psi_{\tilde{\mathbf{K}}}^{(+)}(\mathbf{r}) \times$$

$$\times G_2(t,\tilde{t}') \langle \psi_{\tilde{\mathbf{K}}'}^{(+)} \mid V_+(\tilde{t}') G_{E_1} V_+(\tilde{t}') \mid \varphi_0 \rangle, \quad (47)$$

where the times $\tilde{t}'$ for the first (second) sum are found from Eq. (38) for $v = 1$ ($v = 2$) respectively. The interpretation of the first sum in (47) is analogous to that provided for relation (46), except that at the final stage, the continuum state is formed through the two-photon interaction with the XUV radiation. The partial terms in the second sum reflect the following physical mechanism: the bound electron, having absorbed two photons, passes into a continuum state, where it propagates along a closed trajectory driven by the IR field and forms a continuum state through a single-photon channel of interaction with XUV radiation. It should be noted that, although the determination of higher-order corrections presents no significant difficulties, they are not considered in this work due to the complexity of the final expressions.

4. GENERATION OF RADIATION BY AN ATOM IN SYNCHRONIZED IR AND XUV PULSES

4.1. Generation channels

We will use the obtained expressions for the wave function to determine the radiation generation amplitude by an atom in the field of synchronized, linearly polarized IR and XUV pulses:

$$\mathbf{F}(t) = \mathbf{F}_{IR}(t) + \mathbf{F}_{XUV}(t - \tau), \quad (48)$$

where τ is the time delay between the pulses, defined as the time interval between the peaks of their envelopes. The amplitude of radiation generation is given by Eq. (12) with the substitution:

$$\Psi_{IR}(\mathbf{r},t) \to \Psi(\mathbf{r},t), \quad \tilde{\Psi}_{IR}(\mathbf{r},t) \to \tilde{\Psi}(\mathbf{r},t),$$

where $\tilde{\Psi}(\mathbf{r},t)$ is dual wave function, defined from $\Psi(\mathbf{r},t)$ by the same procedure as $\tilde{\Psi}_{IR}(\mathbf{r},t)$ (see discussion below Eq. (12)).

As shown in the previous section, the wave function $\Psi(\mathbf{r},t)$ is represented as the sum of "slow" ($\Psi^{(s)}(\mathbf{r},t)$) and "fast" ($\Psi^{(r)}(\mathbf{r},t)$) components. Accordingly, the radiation generation amplitude can be written as:

$$\mathcal{D}(\Omega) = \mathcal{D}^{(s)}(\Omega) + \mathcal{D}^{(r)}(\Omega) +$$

$$+ \tilde{\mathcal{D}}^{(r)}(\Omega) + \hat{\mathcal{D}}^{(r)}(\Omega), \quad (49a)$$

$$\mathcal{D}^{(s)}(\Omega) = \int \langle \tilde{\Psi}^{(s)}(\mathbf{r},t) \mid \mathbf{r} \mid \Psi^{(s)}(\mathbf{r},t) \rangle e^{i\Omega t} dt, \quad (49b)$$

$$\mathcal{D}^{(r)}(\Omega) = \int \langle \tilde{\Psi}^{(s)}(\mathbf{r},t) \mid \mathbf{r} \mid \Psi^{(r)}(\mathbf{r},t) \rangle e^{i\Omega t} dt, \quad (49c)$$

$$\tilde{\mathcal{D}}^{(r)}(\Omega) = \int \langle \tilde{\Psi}^{(r)}(\mathbf{r},t) \mid \mathbf{r} \mid \Psi^{(s)}(\mathbf{r},t) \rangle e^{i\Omega t} dt, \quad (49d$$

$$\widehat{\mathcal{D}}^{(r)}(\Omega) = \int \langle \tilde{\Psi}^{(r)}(\mathbf{r},t) \mid \mathbf{r} \mid \Psi^{(r)}(\mathbf{r},t) \rangle e^{i\Omega t} dt, \quad (49e)$$

where each term is discussed in detail below.

The "slow" term $\mathcal{D}^{(s)}(\Omega)$ describes harmonic generation of the XUV field by the atomic system. Considering that $\Psi^{(s)}(\mathbf{r},t)$ is defined by the perturbation series (see Eqs. (33) and (34)), it is evident that $\mathcal{D}^{(s)}(\Omega)$ can be expressed in terms of nonlinear susceptibilities χ_n at the frequencies of the generated harmonics:

$$\mathcal{D}^{(s)}(\Omega) = e^{i\Omega\tau}\sum_{n}\chi_n(\omega_{XUV})F^n_{XUV}f_n(\Omega), \quad (50)$$

$$f_n(\Omega) = \frac{1}{2^n}\int\limits_{-\infty}^{\infty} f^n_{XUV}(t)e^{i\Omega t}dt. \quad (51)$$

It is worth noting that, due to dipole selection rules for centrally symmetric systems, the nonlinear susceptibilities $\chi_n(\omega_{XUV})$ for even number n vanish. However, if we more accurately account for the IR-field effects in the zero-order approximation $\Psi^{(0)}_{IR}(\mathbf{r},t)$, it can be shown that the susceptibilities $\chi_n(\omega_{XUV})$ should be replaced by generalized nonlinear susceptibilities of the atomic system in a static electric field with a strength corresponding to the IR pulse at the delay time τ:

$$\chi_n(\omega_{XUV}) \rightarrow \chi^{(DC)}_n(\omega_{XUV};\mathcal{F}_{DC} = F_{IR}(\tau)). \quad (52)$$

In this case, the prohibition on the generation of even harmonics is lifted, and the spectrum of the generated radiation exhibits peaks corresponding to the frequencies $N\omega_{XUV}$, where N is an integer (see, for example, [39]). Let us consider the "fast" term $\boldsymbol{\mathcal{D}}^{(r)}(\Omega)$ in Eq. (49). Taking into account that the fast part of the wave function in the synchronized IR and XUV pulses is the sum of two terms (see Eq. (36)), we write $\boldsymbol{\mathcal{D}}^{(r)}(\Omega)$ as:

$$\boldsymbol{\mathcal{D}}^{(r)}(\Omega) = \boldsymbol{\mathcal{D}}^{(r,1)}(\Omega) + \boldsymbol{\mathcal{D}}^{(r,2)}(\Omega), \quad (53)$$

where $\boldsymbol{\mathcal{D}}^{(r,i)}(\Omega)(i = 1,2)$ are determined by the corresponding corrections for the fast part of the wave function. Using Eqs. (32) and (37), we obtain $\boldsymbol{\mathcal{D}}^{(r,1)}(\Omega)$ in the form:

$$\boldsymbol{\mathcal{D}}^{(r,1)}(\Omega) = \int \mathcal{D}^{(r,1)}(t)e^{i\Omega t}dt, \quad (54a)$$

$$\mathcal{D}^{(r,1)}(t) = \sum_{\nu=1}^{\infty}\sum_{\tilde{t}'} M_\nu(\tilde{t}')G_\nu\langle\tilde{\Psi}^{(s)} \mid \mathbf{r} \mid \psi^{(+)}_{\tilde{\mathbf{K}}}\rangle, \quad (54b)$$

$$\mid \tilde{\Psi}^{(s)}\rangle = \sum_{\nu}[\widehat{P}_\nu(E_0,-t)\varphi_0]^*, \quad (54c)$$

where $G_\nu \equiv G_\nu(t,\tilde{t}')$is defined in (39), $\tilde{t}'$ are roots of Eq. (38), and $M_\nu(\tilde{t}')$ is the sum of matrix elements describing the ν-photon XUV-induced excitation of the atomic system from the initial state φ_0 to the continuum state $\psi^{(+)}_{\tilde{\mathbf{K}}'}$, considering the re-emission channels. The explicit form of $M_\nu(\tilde{t}')$ can be determined within the perturbation theory using the recurrence relation (30):

$$M_1(\tilde{t}') = \langle\psi^{(+)}_{\tilde{\mathbf{K}}'} \mid \tilde{V}_+ \mid \varphi_0\rangle$$

$$+\langle\psi^{(+)}_{\tilde{\mathbf{K}}'} \mid \tilde{V}_+ G'_{E_0}\tilde{V}_- G_{E_0+\omega_{XUV}}\tilde{V}_+ \mid \varphi_0\rangle + \cdots,$$

$$M_2(\tilde{t}') = \langle\psi^{(+)}_{\tilde{\mathbf{K}}'} \mid \tilde{V}_+ G_{E_0+\omega_{XUV}}\tilde{V}_+ \mid \varphi_0\rangle + \cdots$$

$$M_3(\tilde{t}') = \langle\psi^{(+)}_{\tilde{\mathbf{K}}'} \mid \tilde{V}_+ G_{E_0+2\omega_{XUV}}\tilde{V}_+ G_{E_0+\omega_{XUV}}\tilde{V}_+ \mid \varphi_0\rangle + \cdots,$$

where $\tilde{V}_\pm \equiv V_\pm(\mathbf{r},\tilde{t}')$ (note that for the case of a linearly polarized XUV pulse, $\tilde{V}_+ = \tilde{V}_-$). The third factor in **(**54b**)** (the matrix element $\langle\tilde{\Psi}^{(s)} \mid \mathbf{r} \mid \psi^{(+)}_{\tilde{\mathbf{K}}}\rangle$) determines the amplitude of XUV-assisted recombination into the atomic state at the moment t (see expression **(**34**)**).

The function $\mathcal{D}^{(r,1)}(t)$ rapidly changes with variations in the time t due to the presence of the rapidly oscillating factor $e^{-iS(t,\tilde{t}')}$ in $G_\nu n$. Given that the time interval between ionization and recombination (i.e., the time of electron propagation in the continuum driven by the IR field) is on the order of the IR field period ($|\tilde{t} - \tilde{t}'| \sim T_{IR}$), ionization and recombination cannot occur throughout the duration $\mathcal{T}_{XUV}$ of the attosecond XUV pulse ($\mathcal{T}_{XUV} \ll T_{IR}$). This circumstance allows us to omit all terms in the sum over ν in (54c) except for $\nu = 0$, and to write the recombination amplitude $\langle\tilde{\Psi}^{(s)} \mid \mathbf{r} \mid \psi^{(+)}_{\tilde{\mathbf{K}}}\rangle$ in the lowest-order approximation in F_{XUV} (i.e., assuming $F_{XUV} = 0$ for the state $\tilde{\Psi}^{(s)}$):

$$\langle\tilde{\Psi}^{(s)} \mid \mathbf{r} \mid \psi^{(+)}_{\tilde{\mathbf{K}}}\rangle \approx e^{iE_0 t}\langle\varphi_0 \mid \mathbf{r} \mid \psi^{(+)}_{\tilde{\mathbf{K}}}\rangle. \quad (55)$$

Estimation of the integral (54a) by the stationary phase method leads to the result:

$$\boldsymbol{\mathcal{D}}^{(r,1)}(\Omega) = \sum_{\tilde{t}}\mathcal{D}^{(r,1)}(\tilde{t})e^{i\Omega\tilde{t}}, \quad (56)$$

where the summation is performed over all times that satisfy the equation:

$$\frac{\tilde{\mathbf{K}}^2}{2} = \Omega + E_0, \quad \tilde{\mathbf{K}} = \mathbf{K}(\tilde{t},\tilde{t}'). \quad (57)$$

When solving this equation, one should take into account the implicit dependence of $\tilde{t}' = \tilde{t}'(\tilde{t})$ according to Eq. (38). Based on the obtained analytical relations, it is easy to give a physical interpretation of the radiation generation mechanism described by $\boldsymbol{\mathcal{D}}^{(r,1)}(\Omega)$: the atomic electron absorbs ν XUV photons and passes into the continuum, where it propagates along a closed trajectory driven by of the intense IR field. At the moment of return to the atomic core, the energy gained by the electron is emitted as a photon with the frequency Ω through recombination into the ground state. This generation mechanism is called the “XUV-initiated HHG channel” [44, 46, 71–73].

We represent the dipole moment $\mathcal{D}^{(r,2)}(\Omega)$, determined by the wave function $\Psi^{(r,2)}$, as the sum:

$$\mathcal{D}^{(r,2)}(\Omega) = \mathcal{D}^{(r,2\text{a})}(\Omega) + \mathcal{D}^{(r,2\text{b})}(\Omega), \tag{58}$$

where the partial dipole moments $\mathcal{D}^{(r,2\text{a})}(\Omega)$ and $\mathcal{D}^{(r,2\text{b})}(\Omega)$ correspond to the corrections $\Psi^{(r,2\text{a})}$ and $\Psi^{(r,2\text{b})}$ of the fast part of the wave function (see the discussion of Eq. (41)). Taking into account (42), we write $\mathcal{D}^{(r,2\text{a})}(\Omega)$ as:

$$\mathcal{D}^{(r,2\text{a})}(\Omega) = \int \mathcal{D}^{(r,2\text{a})}(t) e^{i\Omega t}, \tag{59a}$$

$$\mathcal{D}^{(r,2\text{a})}(t) = \sum_s a_s(t) \langle \tilde{\Psi}^{(s)} \,|\, \mathbf{r} \,|\, \Psi^{(+)}_{\mathbf{K}_s} \rangle, \tag{59b}$$

where $\Psi^{(+)}_{\mathbf{K}_s}$ is defined by relation (43). Considering the definition of the dual function $\tilde{\Psi}^{(s)}$, constructed from $\Psi^{(s)}$ (see relation (34)), we express the matrix element in (59b) as:

$$\langle \tilde{\Psi}^{(s)} \,|\, \mathbf{r} \,|\, \Psi^{(+)}_{\mathbf{K}_s} \rangle \approx \sum_n A_n^{(rec)} f^n_{XUV}(t) e^{-in\omega_{XUV} t}, \tag{60}$$

where $A_n^{(rec)} \propto F^n_{XUV}$ is the amplitude of photorecombination with the absorption $(n > 0)$ or emission $(n < 0)$ of **n** XUV photons. Since the function $a_s(t)$ is rapidly oscillating, the integral in (59a) can be evaluated using the stationary phase method. As a result, for the partial amplitude $\mathcal{D}^{(r,2\text{a})}(\Omega)$, we obtain:

$$\mathcal{D}^{(r,2\text{a})}(\Omega) = \sum_{n,s} a_s(t_s) A_n^{(rec)} \times \\ \times f^n_{XUV}(t_s - \tau) e^{i(\Omega - n\omega_{XUV}) t_s}, \tag{61}$$

where the recombination times t_s are found from the stationary phase equation:

$$\frac{\mathbf{K}^2(t_s, t'(t_s))}{2} = \Omega + E_0 - n\omega_{XUV}, \tag{62}$$

and the corresponding ionization times $t'(t_s)$ satisfy Eq. (7) when substituting $t = t_s$. In the following, we will number possible solution pairs of the system of equations (7) and (62) with a single index s: (t_s, t'_s). The analytical relation (61) allows us to give a simple quasiclassical interpretation of the radiation generation mechanism described by the term $\mathcal{D}^{(r,2\text{a})}(\Omega)$: at the moment t'_s, the bound electron tunnels and propagates along a closed trajectory until the moment of recombination t_s. Recombination occurs with the emission of a photon with frequency Ω, simultaneously with the absorption of **n** XUV photons. Moreover, the envelope of the XUV pulse acts as a “temporal separator”, cutting off recombination moments for which the difference $|t_s - \tau|$ exceeds the duration of the XUV pulse. This radiation generation mechanism defines the XUV-assisted HHG channel [52, 53].

Now let us show that the remaining terms $\mathcal{D}^{(r,2\text{b})}(\Omega)$, $\tilde{\mathcal{D}}^{(r)}(\Omega)$ and $\hat{\mathcal{D}}^{(r)}(\Omega)$ are negligibly small. The calculation of the partial dipole moment $\mathcal{D}^{(r,2\text{b})}(\Omega)$, using relations (46), (47), and (33), shows that it is determined by terms that were discarded during the analysis of $\mathcal{D}^{(r,1)}(\Omega)$. In particular, the dipole matrix element of the transition between $\Psi_2^{(r,2\text{b})}$ and $\Psi^{(s)}$ has a second order in F_{XUV} and defines a linear ($\propto F_{XUV}$) correction to the dipole moment in the one-photon XUV-initiated generation channel, through the XUV-interaction at the recombination step (i.e., it includes, along with the the XUV-initiated channel, also the one-photon XUV-assisted recombination channel). Similarly, it can be shown that $\Psi_3^{(r,2b)}$ gives a correction $\propto F^2_{XUV}$ to the one-photon XUV-initiated channel due to the two-photon interaction in the XUV-assisted channel, as well as a correction $\propto F_{XUV}$ to the two-photon XUV-initiated channel via the one-photon XUV-assisted mechanism. These corrections should be discarded due to the significant difference in the time scales between the dynamics of the atomic electron’s interaction with the IR and attosecond XUV pulses: the characteristic time scale between sequential processes of ionization and recombination is comparable to the IR-field period. Therefore, the ionization and recombination stages cannot occur within the duration of a single attosecond XUV pulse.

To estimate the contribution of the dipole moment $\tilde{\mathcal{D}}^{(r)}(\Omega)$, defined by expression (49d), note that it describes the time-inverted process relative to the previously considered generation channels for the term $\mathcal{D}^{(r)}(\Omega)$. This directly follows from the definition of the dual wave function. For example, the generation of radiation in the XUV-assisted channel for $\tilde{\mathcal{D}}^{(r)}(\Omega)$ occurs under the following scenario: the bound electron emits radiation at the frequency Ω, with the simultaneous absorption of n XUV photons. As the result, the electron goes into a virtual state with a larger negative energy and returns to the initial state, interacting with the intense IR field. Since all radiation formation stages occur at negative energy, within the quasiclassical approximation, this mechanism is strongly suppressed, and its contribution is negligibly small (see, for example, the discussion in [63]). Using similar reasoning for the XUV-initiated generation channel, we conclude that it can also be neglected.

Finally, the term $\hat{\mathcal{D}}^{(r)}(\Omega)$ must also be discarded in our consideration, as it is determined by the product of two fast parts of the wave function, and its inclusion exceeds the accuracy established in this analysis. Thus, we have shown that radiation generation by an atomic system, interacting with intense IR radiation and an attosecond XUV pulse, whose duration is much shorter than the IR field period, can occur within the framework of three channels: 1) XUV harmonic generation, defined by the corresponding atomic nonlinear susceptibilities; 2) the XUV-initiated generation channel; 3) the XUV-assisted generation channel.

4.2 Contribution of different radiation generation channels

Let us consider the general properties of the radiation generation channels, such as the position and width of the spectral region $[\Omega_{\min};\Omega_{\max}]$ for a given channel. These properties depend on the characteristics of the atomic target (the energy of the initial bound state) and the parameters of the laser field interacting with the atomic system. The contribution of different generation channels and their spectral overlap is of particular interest.

The frequency interval $[\Omega_{\min};\Omega_{\max}]$ can be determined from the requirement for the existence of real solutions to the saddle-point equations for the classical ionization and recombination times. To find them, we parametrize the electric field of the IR pulse through the vector potential $\mathbf{A}_{IR}(t)$:

$$\mathbf{F}_{IR}(t) = -\frac{\partial \mathbf{A}_{IR}(t)}{\partial t}, \tag{63a}$$

$$\mathbf{A}_{IR}(t) = -\mathbf{e}_x \frac{F_{IR}}{\omega_{IR}} f_{IR}(t)\sin(\omega_{IR} t), \tag{63b}$$

$$f_{IR}(t) = \begin{cases} \cos^2\left(\dfrac{\pi t}{\mathcal{T}_{IR}}\right) & |t| \le \dfrac{\mathcal{T}_{IR}}{2} \\ 0 & |t| \ge \dfrac{\mathcal{T}_{IR}}{2} \end{cases} \tag{63c}$$

where $\mathcal{T}_{IR} = 5T_{IR}$ is the pulse duration, $T_{IR} = 2\pi/\omega_{IR}$. In all numerical calculations, we assume the initial bound state energy $E_0 = -13.6$ eV, corresponding to the ground state of the hydrogen atom.

4.2.1 XUV-assisted channel

For the XUV-assisted generation channel, the ionization times $s_{t'}$ and recombination times s_t satisfy the system of equations (7) and (62):

$$\mathbf{K}_s' \cdot \dot{\mathbf{K}}_s' = 0, \quad \mathbf{K}^2(t_s', t_s) = 2(\Omega + E_0 - n\omega_{XUV}). \tag{64}$$

As seen from Eq. (64), the solution of this system for an arbitrary n can be obtained from the solution for $n = 0$ by a corresponding frequency shift of the generated radiation: $\Omega \to \Omega + n\omega_{XUV}$. Therefore, below we analyze the case $n = 0$, which corresponds to harmonic generation in the absence of the XUV field. The system (64) has real solutions for $\Omega > |E_0|$ and $\Omega < \max \mathbf{K}^2/2 + |E_0| = \alpha_0 u_p + |E_0|$, where $u_p = F_{IR}^2/(4\omega_{IR}^2)$, α_0 is a numerical factor depending on the pulse envelope shape. For example, for a long monochromatic pulse ($f_{IR}(t) \equiv 1$), we obtain $\alpha_0 \approx 3.17$.

Fig. 1 shows the dependence of the frequency Ω of the generated radiation on the recombination times t_j. The color represents the absolute value of the tunneling factor $a_j^{(tun)}$, which enters the expression (14b) for the partial HHG amplitude for the IR field. It is seen from the figure that for fixed parameters of the laser pulse, the number of solutions of system (64) increases with decreasing Ω, which leads to the formation of a complex interference structure in the plateau region [17]. In the vicinity of the global maximum for Ω (i.e., the cutoff of the IR-induced HHG plateau), only two solutions exist, determining the well-known interference oscillations of the HHG yield near the cutoff region [74, 75].

4.2.2 XUV-initiated channel

For the XUV-initiated channel (consisting of an ν-photon transition of the electron from the ground state to the continuum, its laser-driven propagation, and subsequent recombination), the ionization and recombination times are determined by the following system of equations:

$$\frac{\tilde{\mathbf{K}}'^2}{2} = E_0 + \nu\omega_{XUV}, \tag{65a}$$

$$\frac{\tilde{\mathbf{K}}^2}{2} = E_0 + \Omega, \tag{65b}$$

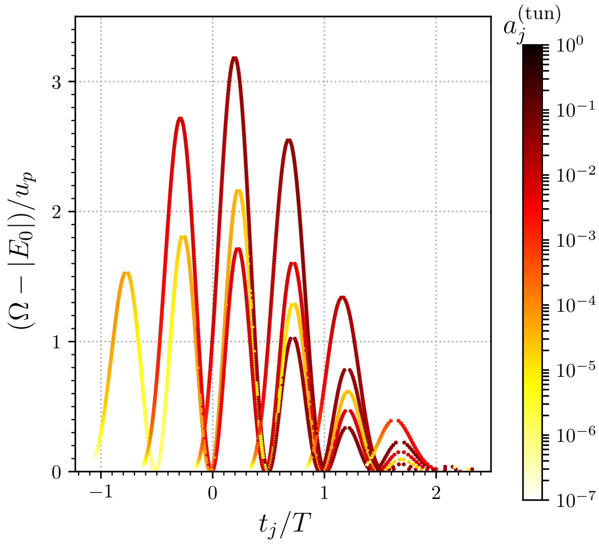

Fig. 1. Dependence of the recombination time on the frequency of the generated radiation for an IR pulse with a carrier frequency $\omega = 1$ eV and a peak intensity $2 \cdot 10^{14}$ W/cm². The color represents the value of the tunneling factor (10), calculated for the ionization and recombination times satisfying the system of equations (64) $u_p = 26.89$ eV. $|E_0| = 13.65$ eV.

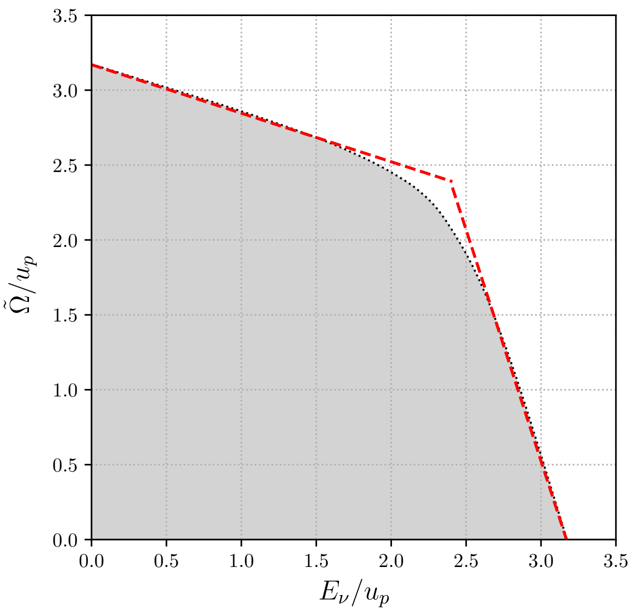

Fig. 2. Region of existence for solutions of the saddle-point equations (65). The dark gray area represents the parameter region obtained from the numerical solution, while the red dashed line shows the linear law (67).

where $\tilde{\mathbf{K}}' = \mathbf{K}'(\tilde{t},\tilde{t}')$, $\tilde{\mathbf{K}} = \mathbf{K}(\tilde{t},\tilde{t}')$.

Equation (65a) has real solutions under the following necessary condition:

$$\nu\omega_{XUV} \leqslant \max\left(|E_0| + \frac{\tilde{\mathbf{K}}'^2}{2}\right) = |E_0| + \alpha_0 u_p. \quad (66)$$

To determine the boundaries of the spectral region $[\Omega_{\min};\Omega_{\max}]$ of classically allowed frequencies of the generated radiation, note that the system of equations (65) is invariant with respect to the replacement $(\tilde{\mathbf{K}}', E_\nu) \leftrightarrow (\tilde{\mathbf{K}}, \tilde{\Omega})$, where $\tilde{\Omega} = \Omega + E_0$. The maximum values $\tilde{\mathbf{K}}'^2/2$ and $\tilde{\mathbf{K}}^2/2$ are identical due to the obvious symmetry in the dependence of $\mathbf{K}(t,t')$ and $\mathbf{K}'(t,t')$ on the times t, t' (see Eqs. (6) and (8)). Therefore, in the plane of the variables $\tilde{\Omega}$ and E_ν, the desired region of real solutions (or classically allowed energies $\tilde{\Omega}$ and E_ν is symmetric with respect to the line $\tilde{\Omega} = E_\nu$. Moreover, since the momenta $\mathbf{K}$ and $\mathbf{K}'$ are proportional to F_{IR}/ω_{IR}, the region of real solutions in the coordinates $\tilde{\Omega}$, E_ν scales by the magnitude u_p. From the above, it follows that the boundary of classically allowed energies can be expressed using a symmetric function $g(x,y) = g(y,x)$ of the two arguments $x = \tilde{\Omega}/u_p$ and $y = E_\nu/u_p$ in the form of the following equation:

$$g\left(\frac{\tilde{\Omega}}{u_p}, \frac{E_\nu}{u_p}\right) = 0.$$

Fig. 2 shows the region of classically allowed energies $\tilde{\Omega}$ and E_ν, obtained from the numerical analysis of the system of equations (65). The desired region is well approximated by two straight lines [76]:

$$g\left(\frac{\tilde{\Omega}}{u_p}, \frac{E_\nu}{u_p}\right) \approx \begin{cases} \dfrac{\tilde{\Omega}}{u_p} + \beta_0 \dfrac{E_\nu}{u_p} - \alpha_0, & \tilde{\Omega} > E_\nu, \\ \dfrac{E_\nu}{u_p} + \beta_0 \dfrac{\tilde{\Omega}}{u_p} - \alpha_0, & \tilde{\Omega} < E_\nu \end{cases} \quad (67)$$

where

$$\beta_0 = F_{IR}(t_0')\,/\,F_{IR}(t_0),$$

t_0' and t_0 are ionization and recombination times, corresponding to the global maximum of $\tilde{\mathbf{K}}^2/2$ (for the monochromatic field $\beta_0 = 0.324$).

The dependence of the solutions of the system of equations (65) on the frequency of the generated radiation Ω is shown in Fig. 3. Each pair of solutions $(\tilde{t}',\tilde{t})$ is represented by a point, the color of which corresponds to a specific value of ω_{XUV}. As can be seen from the presented figure, as well as from the above estimate (66), the number of real roots

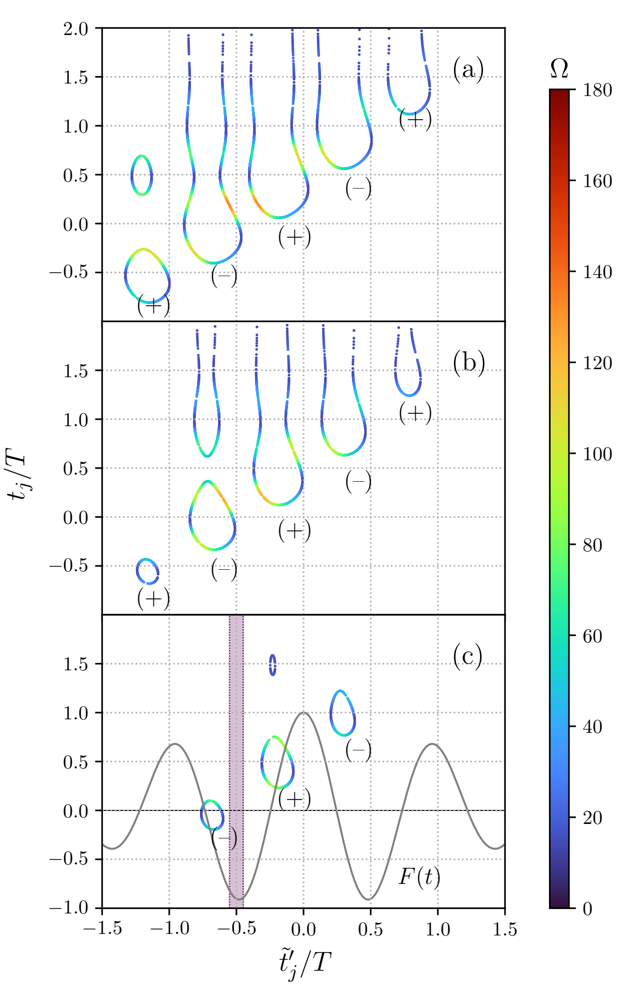

Fig. 3. Solutions of the system of equations (65) for the classical ionization times t'_+ and recombination times t_+ in the case of single-photon ionization ($\nu = 1$) and various values of the XUV photon energy: (a) $\omega_{XUV} = 40$ eV, (b) $\omega_{XUV} = 60$ eV, (c) $\omega_{XUV} = 100$ eV. The shaded purple area represents the duration of the XUV pulse. The initial-state energy, carrier frequency of the IR pulse, XUV pulse duration, and the time delay between the pulses are the same as in Fig. 1, while the peak intensity of the IR pulse is $I = 3 \cdot 10^{14}$ W/cm^2. The signs (±) indicate the direction of the instantaneous momentum $\tilde{\mathbf{K}}$ of the electron at the moment of ionization relative to the polarization vector $\mathbf{e}_x$ of the IR field: (+) for the case $(\tilde{\mathbf{K}} \cdot \mathbf{e}_x) > 0$ and (−) for the case $(\tilde{\mathbf{K}} \cdot \mathbf{e}_x) < 0$. The black line represents the profile of the IR field intensity in arbitrary units.

of the system (65) decreases with the increase of ω_{XUV}, while the region of possible values for the ionization and recombination times shrinks (see the regions bounded by closed curves in Fig. 3). We remind that in the theory being developed, the interaction of the XUV pulse with the atomic system is determined by the specific moments of ionization and recombination (see Section 3), which define the closed trajectory of the free electron in the IR field. Therefore, at certain time delays, the considered generation channel can be suppressed due to the lack of overlap between the solution region of the system (65) and the time interval of interaction with the XUV pulse. For example, in Fig. 3c, it is shown that for an XUV pulse with a time delay $\tau = -0.5T$, the region of acceptable values for $\tilde{t}'$ does not intersect with the time interval of the XUV pulse duration.

Dependence of the generated radiation frequency on the recombination times for all the discussed generation channels is shown in Fig. 3. The regions corresponding to elastic scattering of the XUV photon by the atomic system (Rayleigh scattering) and the second harmonic generation are indicated by the horizontal dashed lines in the figure (solid bold horizontal lines correspond to $\Omega = \omega_{XUV}$ and $\Omega = 2\omega_{XUV}$). At IR-pulse intensities of $I \gtrsim 2 \cdot 10^{14}$ W/cm^2, we observe a spectral overlap between the harmonic generation channel in the IR field (black bold lines in Fig. 3) and the elastic scattering channel of the XUV photon, leading to the specific oscillations in the harmonic generation spectrum [60]. As the IR pulse intensity increases, overlap with the XUV harmonic generation channels occurs (see Fig. 3(c), where overlap with the second XUV harmonic generation channel is observed at $I = 4 \cdot 10^{14}$ W/cm^2). We note, that for the occurrence of interference between different radiation generation channels, necessary conditions are spectral overlap of the channels and comparable generation probabilities within the desired channels. The XUV-initiated channels (green and orange lines) overlap spectrally only with the harmonic generation channel in the single IR pulse. Moreover, as seen in Fig. 3, as the number of photons in the XUV-initiated channel increases, the spectral overlap region shrinks, which is obviously related to the reduced energy gain by the electron during its propagation in the IR-field after absorbing ν XUV photons (see Fig. 2). Thus, the observation of XUV-initiated generation channels with $\nu > 1$ is difficult due to suppression by the more intense HHG channel in the absence of the XUV pulse and is possible only with a significant increase in the XUV-field intensity. For $\nu = 1$, the XUV-initiated channel can be distinguished under the orthogonal geometry of the IR and XUV pulses [77]. In contrast, the XUV-assisted channels (thin gray lines in Fig. 3) contribute to the generation of higher-frequency radiation, forming sequential plateau-like structures in the HHG spectra [53]. Typically, the XUV-assisted channels interfere with the harmonic generation channels of the XUV radiation

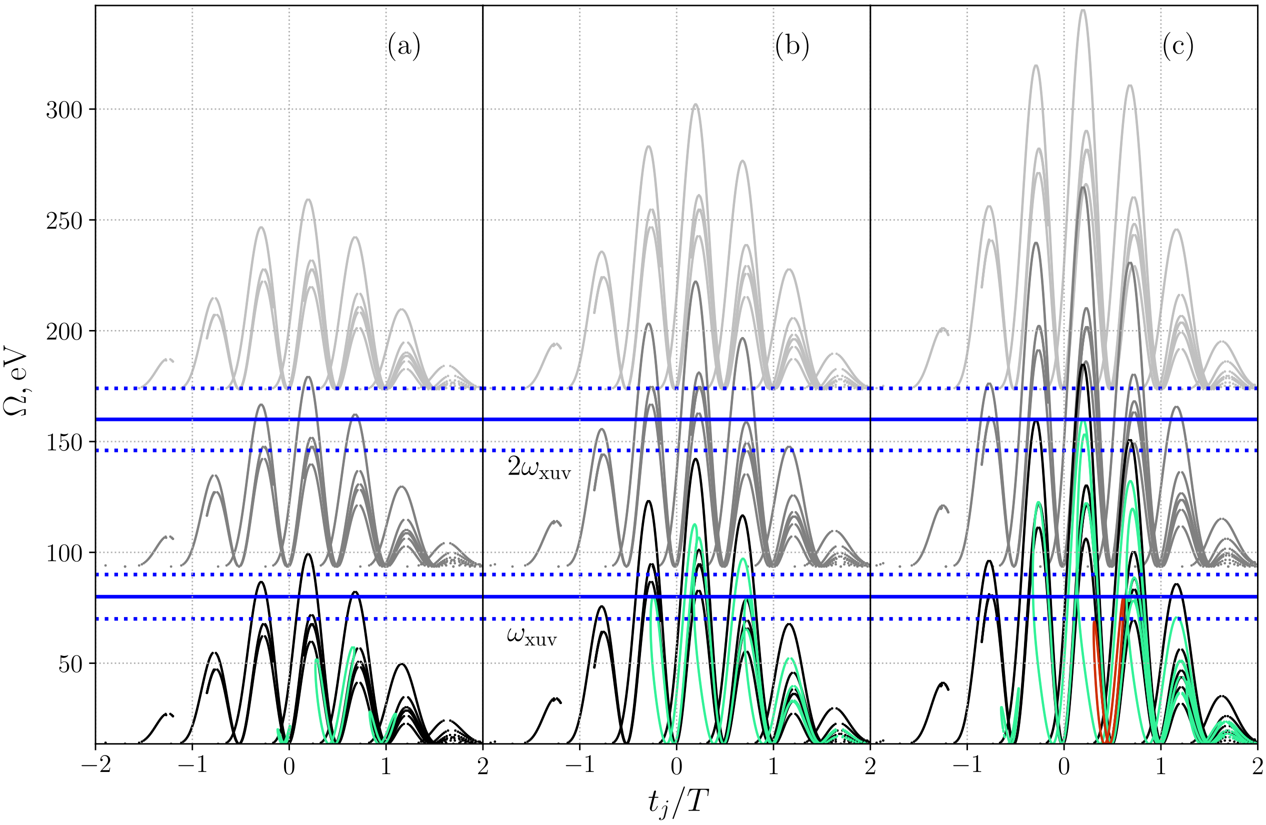

Fig. 4. Spectrograms of generation channels for different peak intensities of the IR pulse: (a) $I = 2 \cdot 10^{14}$ W/cm^2, (b) $3 \cdot 10^{14}$ W/cm^2 and (c) $4 \cdot 10^{14}$ W/cm^2. Black lines show the HHG channel in the absence of the XUV field. Gray lines represent the XUV-assisted channel with the absorption of one and two XUV photons. Green lines (orange lines) represent the XUV-initiated channel with the absorption of one (two) XUV photons. The solid horizontal lines indicate the values of $\Omega = N\omega_{XUV}$ ($N = 1,2$), while the dashed horizontal lines show the boundaries of the spectral regions for the first and second XUV harmonics. The XUV photon energy is $\omega_{XUV} = 80$ eV, and the initial-state energy, carrier frequency of the IR field, and XUV pulse envelope parameters are the same as in Fig. 1.

[39]. Note that it is possible to select conditions for spectral overlap between the harmonic generation channel in the single IR pulse and the XUV-assisted and XUV-initiated channels [see Fig. 4(c)].

5. CONCLUSION

In this work, an adiabatic approach has been developed for analyzing the interaction effects of an IR-dressed atomic system with a short (attosecond) XUV pulse. The nonlinear effects due to XUV interaction result in the emergence of additional XUV-induced radiation generation channels. Depending on the nature of the XUV pulse's influence on the atom, these channels can be classified into three types. The first one is the XUV-induced modification of nonlinear susceptibilities of the atomic system. For initially non-polarized targets, the odd-order susceptibilities (e.g., atomic polarizability, describing Rayleigh scattering of the XUV photon [60], or the third-order susceptibility, responsible for third XUV harmonic generation) do not vanish in the absence of the IR field. Thus, at moderate field intensities, they can be approximated by the susceptibilities of the free atom. In contrast, even-order susceptibilities (e.g., those describing the XUV rectification effect [61] or the second XUV harmonic generation [39]) vanish when the IR field is switched off, as they are caused by the IR-induced symmetry breaking of the atomic state. The first type of channels has been thoroughly studied in the works cited above.

The main focus of this study is on the second and third types of channels – the XUV-induced ionization channels, involving the absorption of XUV photons during the first stage of the three-step rescattering mechanism, and the XUV-assisted recombination channels, where XUV photons are absorbed at the moment the electron returns to the atomic core. Analysis of the contributions of partial amplitudes associated with various closed classical trajectories of the electron in the IR field, in accordance with the described XUV-initiated and XUV-assisted channels, revealed that for moderate IR pulse intensities, the spectral region of XUV-initiated channels overlaps only with the harmonic spectrum of the IR field in the absence of the XUV pulse, while the probability of interference with XUV harmonic generation channels is negligibly small. In contrast, XUV photon absorption during recombination (XUV-assisted channel) significantly expands the spectrum of the generated radiation, enabling the interference of different generation channels.

It is worth noting that for short XUV pulses, the energy range of the generation channels strongly depends on the time delay between the XUV and IR pulses. For example, in the case of high XUV photon energies, there are delay intervals where the XUV-initiated generation channel is suppressed. It is important to emphasize that interference phenomena, caused by the spectral overlap of different XUV-induced generation channels with the IR-field HHG channel, are key to a deeper understanding of atomic photoprocesses occurring in the field of synchronized XUV and IR pulses. These phenomena can also form the basis for optical methods to extract the temporal profile of the IR pulse from the measured generation spectra [39, 77, 78].

FUNDING

This work was supported by the Russian Science Foundation (theory of radiation generation by atoms in IR and XUV pulses, Project No. 22-12-00223) and by a grant from the Ministry of Science and Higher Education of the Russian Federation (general perturbation theory in XUV-interaction for the IR-dressed atom, Project No. 075-15-2021-1351).

REFERENCES

1. *J. Caillat, J. Zanghellini, M. Kitzler, O. Koch, W. Kreuzer, and A. Scrinzi*, Phys. Rev. A **71**, 012712 (2005).
2. *D. Bauer and P. Koval*, Comp. Phys. Comm. **174**, 396 (2006).
3. *D. A. Telnov and S.-I. Chu*, Phys. Rev. A **80**, 043412 (2009).
4. *L. Greenman, P. J. Ho, S. Pabst, E. Kamarchik, D. Mazziotti, and R. Santra*, Phys. Rev. A **82**, 023406 (2010).
5. *D. A. Telnov, K. E. Sosnova, E. Rozenbaum, and S.-I. Chu*, Phys. Rev. A **87**, 053406 (2013).
6. *T. Sato and K. L. Ishikawa*, Phys. Rev. A, **88**, 023402 (2013).
7. *S. Patchkovskii and H. Muller*, Comp. Phys. Comm. **199**, 153 (2016).
8. *V. Tulsky and D. Bauer*, Comp. Phys. Comm. **251**, 107098 (2020).
9. *A. A. Romanov, A. A. Silaev, M. V. Frolov, and N. V. Vvedenskii*, Phys. Rev. A **101**, 013435 (2020).
10. *V. V. Strelkov*, Phys. Rev. A **74**, 013405 (2006).
11. *O. I. Tolstikhin, T. Morishita, and S. Watanabe*, Phys. Rev. A **81**, 033415 (2010).
12. *O. I. Tolstikhin and T. Morishita*, Phys. Rev. A **86**, 043417 (2012).
13. *Y. Okajima, O. I. Tolstikhin, and T. Morishita*, Phys. Rev. A **85**, 063406 (2012).
14. *M. V. Frolov, N. L. Manakov, A. A. Minina, A. A. Silaev, N. V. Vvedenskii, M. Y. Ivanov, and A. F. Starace*, Phys. Rev. A **99**, 053403 (2019).
15. *A. V. Flegel, N. L. Manakov, A. V. Sviridov, M. V. Frolov, L. Geng, and L.-Y. Peng*, Phys. Rev. A **102**, 063119 (2020).
16. *A. V. Sviridov, M. V. Frolov, S. V. Popruzhenko, L. Geng, and L.-Y. Peng*, Phys. Rev. A **106**, 033117 (2022).
17. *A. V. Flegel, N. L. Manakov, I. V. Breev, and M. V. Frolov*, Phys. Rev. A **104**, 033109 (2021).
18. *A. A. Romanov, A. A. Silaev, T. S. Sarantseva, M. V. Frolov, and N. V. Vvedenskii*, New J. Phys. **23**, 043014 (2021).
19. *D. B. Milosevic and F. Ehlotzky*, Adv. At., Mol. Opt. Phys., **49**, 373 (2003).
20. *W. Becker, F. Grasbon, R. Kopold, D. B. Milosevic, G. G. Paulus, and H. Walther*, Adv. At. Mol. Opt. Phys. **48**, 35 (2002).
21. *A. Galstyan, O. Chuluunbaatar, A. Hamido, Y. V. Popov, F. Mota-Furtado, P. F. O'Mahony, N. Janssens, F. Catoire, and B. Piraux*, Phys. Rev. A **93**, 023422 (2016).
22. *Y. Popov, A. Galstyan, F. Mota-Furtado, P. F. O'Mahony, and B. Piraux*, ' Eur. Phys. J. D **71**, 93 (2017).
23. *L. V. Keldysh*, JETP **20**, 1307 (1965).
24. *M. V. Fedoruk*, Saddle point method, Nauka, Moscow (1977) [in Russian].
25. *P. Salieres, B. Carre, L. Le Deroff, F. Grasbon, G. G. Paulus, H. Walther, R. Kopold, W. Becker, D. B. Milosevic, A. Sanpera, and M. Lewenstein*, Science **292**, 902 (2001).
26. *D. B. Milosevic*, Phys. Rev. A **96**, 023413 (2017).
27. *P. B. Corkum*, Phys. Rev. Lett. **71**, 1994 (1993).

28. *W. Becker, A. Lohr, and M. Kleber*, J. Phys. B: At. Mol. Opt. Phys. **27**, L325 (1994).

29. *M. V. Frolov, N. L. Manakov, T. S. Sarantseva, M. Y. Emelin, M. Y. Ryabikin, and A. F. Starace*, Phys. Rev. Lett. **102**, 243901 (2009).

30. *M. V. Frolov, N. L. Manakov, and A. F. Starace*, Phys. Rev. A **82**, 023424 (2010).

31. *A. D. Shiner, B. E. Schmidt, C. Trallero-Herrero, H. J. Wörner, S. Patchkovskii, P. B. Corkum, J.-C. Kieffer, F. Legare, and D. M. Villeneuve*, Nat. Phys. **7**, 464 (2011).

32. *A. D. Shiner, B. E. Schmidt, C. Trallero-Herrero, P. B. Corkum, J.-C. Kieffer, F. L'egar'e, and D. M. Villeneuve*, J. Phys. B: At. Mol. Opt. Phys. **45**, 74010 (2012).

33. *V. N. Ostrovsky and D. A. Telnov*, J. Phys. B: At. Mol. Opt. Phys. **20**, 2397 (1987).

34. *V. N. Ostrovsky and D. A. Telnov*, J. Phys. B: At. Mol. Opt. Phys. **20**, 2421 (1987).

35. *M. Pont, R. Shakeshaft, and R. M. Potvliege*, Phys. Rev. A **42**, 6969 (1990).

36. *D. A. Telnov*, J. Phys. B: At. Mol. Opt. Phys. **24**, 2967 (1991).

37. *M. Pont, R. M. Potvliege, R. Shakeshaft, and Z. Teng*, Phys. Rev. A **45**, 8235 (1992).

38. *A. V. Flegel and M. V. Frolov*, J. Phys. A: Math. Theor. **56**, 505304 (2023).

39. *A. A. Romanov, A. A. Silaev, N. V. Vvedenskii, I. V. Breev, A. V. Flegel, and M. V. Frolov*, Phys. Rev. A **106**, 063101 (2022).

40. *K. Ishikawa*, Phys. Rev. Lett. **91**, 043002 (2003).

41. *K. L. Ishikawa*, Phys. Rev. A **70**, 013412 (2004).

42. *K. Schiessl, E. Persson, A. Scrinzi, and J. Burgdörfer*, Phys. Rev. A **74**, 053412 (2006).

43. *S. V. Popruzhenko, D. F. Zaretsky, and W. Becker*, Phys. Rev. A **81**, 063417 (2010).

44. *K. J. Schafer, M. B. Gaarde, A. Heinrich, J. Biegert, and U. Keller*, Phys. Rev. Lett. **92**, 023003 (2004).

45. *M. B. Gaarde, K. J. Schafer, A. Heinrich, J. Biegert, and U. Keller*, Phys. Rev. A 72, 013411(2005).

46. *J. Biegert, A. Heinrich, C. P. Hauri, W. Kornelis, P. Schlup, M. P. Anscombe, M. B. Gaarde, K. J. Schafer, and U. Keller*, J. Mod. Opt. **53**, 87 (2006).

47. *C. Figueira de Morisson Faria, P. Salieres, P. Villain, and M. Lewenstein*, Phys. Rev. A **74**, 053416 (2006).

48. *G.-T. Zhang, J. Wu, C.-L. Xia, and X.-S. Liu*, Phys. Rev. A **80**, 055404 (2009).

49. *M. R. Miller, C. Hernandez-Garcia, A. Jaron-Becker, and A. Becker*, Phys. Rev. A **90**, 053409 (2014).

50. *P. B. Corkum, N. H. Burnett, and M. Y. Ivanov*, Opt. Lett. **19**, 1870 (1994).

51. A. Fleischer and N. Moiseyev, Phys. Rev. A 77, 010102 (2008).

52. *A. Fleischer*, Phys. Rev. A **78**, 053413 (2008).

53. *T. S. Sarantseva, M. V. Frolov, N. L. Manakov, A. A. Silaev, N. V. Vvedenskii, and A. F. Starace*, Phys. Rev. A **98**, 063433 (2018).

54. *C. Buth, F. He, J. Ullrich, C. H. Keitel, and K. Z. Hatsagortsyan*, Phys. Rev. A **88**, 033848 (2013).

55. *A. C. Brown and H. W. van der Hart*, Phys. Rev. Lett. **117**, 093201 (2016).

56. *J.-A. You, J. M. Dahlstr..om, and N. Rohringer*, Phys. Rev. A **95**, 023409 (2017).

57. *J. Leeuwenburgh, B. Cooper, V. Averbukh, J. P. Marangos, and M. Ivanov*, Phys. Rev. Lett. **111**, 123002 (2013).

58. *J. Leeuwenburgh, B. Cooper, V. Averbukh, J. P. Marangos, and M. Ivanov*, Phys. Rev. A **90**, 033426 (2014).

59. *C. Buth, M. C. Kohler, J. Ullrich, and C. H. Keitel*, Opt. Lett. **36**, 3530 (2011).

60. *A. A. Romanov, A. A. Silaev, N. V. Vvedenskii, A. V. Flegel, and M. V. Frolov*, Opt. Lett. **47**, 3147 (2022).

61. *A. V. Flegel and M. V. Frolov*, Phys. Rev. Lett. **131**, 243202 (2023).

62. *A. A. Minina, M. V. Frolov, A. N. Zheltukhin, and N. V. Vvedenskii*, Quant. Elect. **47**, 216 (2017).

63. *M. Y. Kuchiev and V. N. Ostrovsky*, Phys. Rev. A **60**, 3111 (1999).

64. *M. V. Frolov, A. V. Flegel, N. L. Manakov, and A. F. Starace*, Phys. Rev. A **75**, 063407 (2007).

65. *R. M. Potvliege and R. Shakeshaft*, Phys. Rev. A **40**, 3061 (1989).

66. *N. L. Manakov, M. V. Frolov, A. F. Starace, and I. I. Fabrikant*, J. Phys. B: At. Mol. Opt. Phys. **33**, R141 (2000).

67. *N. L. Manakov and A. G. Fainshtein*, Theoret. and Math. Phys. **48**, 815 (1981).

68. *E. A. Pronin, A. F. Starace, M. V. Frolov, and N. L. Manakov*, Phys. Rev. A **80**, 063403 (2009).

69. *P. W. Langhoff, S. T. Epstein, and M. Karplus*, Rev. Mod. Phys. **44**, 602 (1972).

70. *N. L. Manakov, V. D. Ovsiannikov, and L. P. Rapoport*, Phys. Rep. **141**, 320 (1986).

71. *G. Gademann, F. Kelkensberg, W. K. Siu, P. Johnsson, M. B. Gaarde, K. J. Schafer, and M. J. J. Vrakking*, New J. Phys. **13**, 033002 (2011).

72. *D. Azoury, M. KrGjger, G. Orenstein, H. R. Larsson, S. Bauch, B. D. Bruner, and N. Dudovich*, Nat. Comm. **8**, 1453 (2017).

73. *M. Krüger, D. Azoury, B. D. Bruner, and N. Dudovich*, Appl. Sci. **9**, 378 (2019).

74. *M. V. Frolov, N. L. Manakov, T. S. Sarantseva, and A. F. Starace*, J. Phys. B: At. Mol. Opt. Phys. **42**, 035601 (2009).

75. *M. V. Frolov, N. L. Manakov, A. M. Popov, O. V. Tikhonova, E. A. Volkova, A. A. Silaev,* *N. V. Vvedenskii, and A. F. Starace*, Phys. Rev. A **85**, 033416 (2012).

76. *A. V. Flegel, M. V. Frolov, A. N. Zheltukhin, and N. V. Vvedenskii*, Quant. Electron. **47**, 222 (2017).

77. *T. S. Sarantseva, A. A. Romanov, A. A. Silaev, N. V. Vvedenskii, and M. V. Frolov*, Phys. Rev. A **107**, 023113 (2023).

78. *A. A. Romanov, A. A. Silaev, T. S. Sarantseva, A. V. Flegel, N. V. Vvedenskii, and M. V. Frolov*, Opt. Lett. **48**, 3583 (2023).